Bioorganic & Medicinal Chemistry 19 (2011) 4887–4894

Contents lists available at ScienceDirect

Bioorganic & Medicinal Chemistry

journal homepage: www.elsevier.com/locate/bmc

Polyfluorinated bipyridine cisplatins manipulate cytotoxicity through the induction of S-G_2/M arrest and partial intercalation mechanism

Tzu Ting Chang [a], Shivaji V. More [a], Norman Lu [b,*], Jyun-Wei Jhuo [b], Yi-Chuan Chen [b], Shu-Chuan Jao [c], Wen-Shan Li [a,d,*]

[a] Institute of Chemistry, Academia Sinica, Taipei 115, Taiwan
[b] Department of Molecular Science and Engineering, National Taipei University of Technology, Taipei 106, Taiwan
[c] Institute of Biological Chemistry, Academia Sinica, Taipei 115, Taiwan
[d] Doctoral Degree Program in Marine Biotechnology, National Sun Yat-Sen University, Kaohsiung 804, Taiwan

ARTICLE INFO

Article history:
Received 25 March 2011
Revised 23 June 2011
Accepted 23 June 2011
Available online 28 June 2011

Keywords:
Antiproliferative effect
Anticancer agents
Cell cycle progression
DNA intercalation mechanism
Polyfluorinated bipyridine cisplatin complexes

ABSTRACT

A series of polyfluorinated bipyridine cisplatins **2–6** were prepared, characterized, and evaluated for their in vitro cytotoxicities against a panel of human cancer cell lines, MCF7 (breast adenocarcinoma), MDA-MB-231 (breast adenocarcinoma) and A549 (lung adenocarcinoma). The results show that a correlation between the relative order of lipophilicity of complexes **2–4** and their cytotoxicity is established by following the trend: **4** > **2** > **3**. Complex **4**, which is the most active compound in the series, was found to be a more effective and selective anticancer agent than cisplatin. Complex **4** inhibited cancer cell proliferation by partial intercalation to DNA, which subsequently resulted in induction of S-G2/M arrest and apoptosis.

1. Introduction

Polyfluorinated compounds, the artificially producing products exhibiting lipophilicity and metabolic stability, perform a myriad functions such as low surface tension[1,2] and molecular recognition to serve as a unique constituent of liquid crystals,[3–6] surfactants,[7–16] enzyme inhibitors[17–23] and antiviral/anticancer agents[24–29] in industry and pharmaceutical company. Furthermore, many polyfluorinated compounds possess capability of self-assembly to enhance global stability which is crucial to a success of fluorous technology in biological applications.[30]

Cisplatin, carboplatin and their analogs are utilized as anticancer drugs in the worldwide chemotherapy treatment. However the adverse effects and drug resistances remain challenging. Many platinum complexes have been made and evaluated at the stages of clinical trials recently to overcome these problems.[31] Naturally, every therapeutic drug interacts with its bio-targets to remediate undesirable disease condition associated with various side effects and drug resistances. Enhancing the quality of life of patients is generally a prerequisite for proper chemotherapy. Therefore, there is particular interest in the search of anticancer agents that can minimize side effects and enhance the therapeutic effects.

2,2′-Bipyridine, one of the pyridyl compounds, operates as a bidentate chelating ligand for metal binding. The UV–Vis absorption properties of this class of bipyridyl metal complexes have been utilized to monitor the interaction processes with DNA. In addition, the molecular nature of bipyridyl metal complex provides a square-planar geometry to intercalate with DNA. These evidences suggest that DNA does represent the potent target, perhaps, for many bipyridyl metal complexes. Recent progresses have emphasized the antiproliferative effects and molecular mechanisms from diverse metals, gold(III),[32,33] copper(II/I),[34,35] palladium(II),[36,37] rhodium(III),[38] ruthenium (II),[39,40] zinc(II)[41] and platinum(II),[42,43] with bipyridyl ligands. In particular, the fluorinated bipyridine cisplatin analog with terminal trifluoromethyl moiety is more potent than that with terminal methoxy group,[44] inspiring us to pursue research on the effect of various polyfluorinated chain lengths on tumor-specific cytotoxicity.

Herein, we describe the synthesis of a series of bipyridine cisplatin analogs with different polyfluorinated side chains at the 4, 4′ positions. We propose to test the ability of polyfluorinated bipyridine cisplatins **2–6** (Chart 1) to inhibit growth of human

* Corresponding authors. Tel.: +886 (2) 27712171x2417; fax: +886 (2) 227317174 (N.L.); tel.: +886 (2) 27898662; fax: +886 (2) 27831237 (W.-S.L.).
E-mail addresses: normanlu@ntut.edu.tw (N. Lu), wenshan@chem.sinica.edu.tw (W.-S. Li).

0968-0896/$ - see front matter © 2011 Elsevier Ltd. All rights reserved.
doi:10.1016/j.bmc.2011.06.065

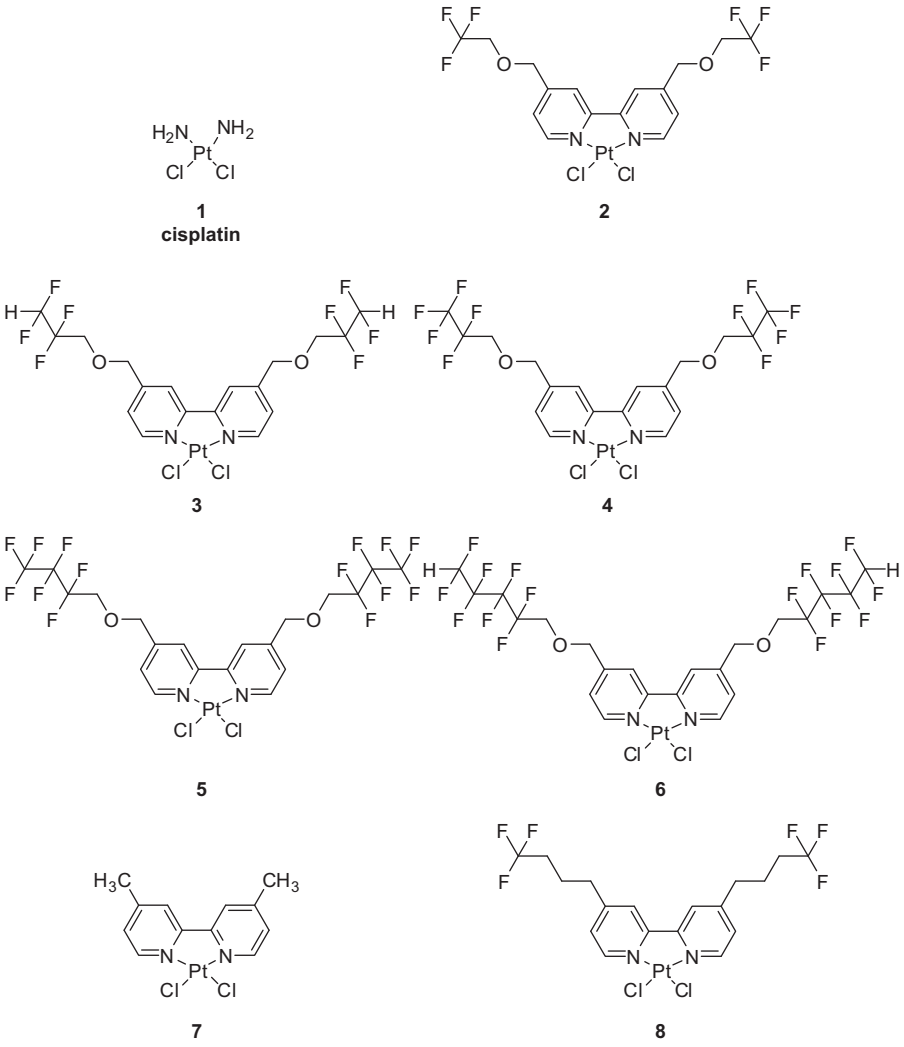

Chart 1.

cancer-cell lines, namely MCF7, MDA-MB-231(breast adenocarcinoma) and A549 (lung adenocarcinoma). To study the antiproliferative action, the most effective complex, **4**, was chosen. Complex **4**-induced cytotoxicity in MDA-MB-231 cells via cell cycle progression and DNA interaction studies was reported.

2. Experimental section

2.1. General

The gas chromatographic/mass spectrometric data were taken using an Agilent 6890 Series gas chromatograph with a series 5973 mass selective detector. The GC monitoring employed a HP 6890 GC using a 30 m × 0.250 mm HP-5 capillary column with a 0.25 μm stationary phase film thickness. The electron ionization (EI) mode is used to study the fluorous ligands.[45,47,48] Infrared spectra were obtained on a Perkin Elmer RX I FT-IR Spectrometer. NMR spectra were recorded on Bruker AM 500 using 5 mm sample tubes. The residual peaks of $CDCl_3$, deuterated Me_2SO and deuterated DMF were used as the reference peaks for both ^1H and ^{13}C NMR spectra; that of Freon® 11 ($CFCl_3$) for ^{19}F-NMR spectra. Fast atom bombardment (FAB) mass spectroscopy analysis was provided by the staff of the National Central University (Taiwan) Mass Spectrometry Laboratory.

2.2. Preparation of platinum complexes

Chemicals, reagents, and solvents employed were commercially available and used as received. The CF_3CH_2OH, $HCF_2CF_2CH_2OH$, $C_2F_5CH_2OH$, $C_3F_7CH_2OH$ and $HCF_2(CF_2)_3CH_2OH$ were purchased from Aldrich or SynQuest. Platinum complex **7** was prepared by using the same protocol as that described in the report of Carper and co-workers.[27]

Platinum complexes: [$PtCl_2$(4,4′-bis($R_fCH_2OCH_2$)-2,2′-bpy)] where R_f = *n*-CF_3 (**2**, **Pt-3F**), HCF_2CF_2 (**3**, **Pt-4F**), *n*-C_2F_5 (**4**, **Pt-5F**), *n*-C_3F_7 (**5**, **Pt-7F**), $HCF_2(CF_2)_3$ (**6**, **Pt-8F**).

Equal molar [$PtCl_2(CH_3CN)_2$] (0.144 mmol; 50.1 mg) and ligand (0.144 mmol) were charged into a round bottomed flask, and CH_2Cl_2 (8 mL) was added as the solvent. The color of solution changed from pale yellow to bright yellow after mixing for several minutes. The solution was further stirred at room temperature for 24 h before the solvents and volatiles were removed under vacuum. The resulting bright yellow solid was collected as spectroscopically pure product **2–6**. Their analytical data are listed below. Take compound **2,** for example, **2** was soluble in polar solvent (e.g., DMF), but insoluble in methanol. Accordingly, the recrystallization proceeded with dissolution of **2** in DMF to form a yellow solution, to which a methanol overlayer (5 cm^3) was added. Then, solvent diffusion over a period of 10 days at 25 °C afforded pale yellow crystals of **2**.

2.2.1. Preparation of Pt-3F (2)

Analytical data of ***Pt-3F*** *(**2**): Yield* 83.8%. ^{1}H NMR (500 MHz, 298 K, DMSO-d_6): δ 9.41 (d, J_{HH} = 6.0 Hz, 2H, H_6), 8.44 (s, 2H, H_3), 7.77 (d, J_{HH} = 6.0 Hz, 2H, H_5), 4.89 (s, 4H, bpy-CH_2), 4.30 (q, J_{FH} = 9.2 Hz, 4H, –OCH_2CF$_3$). ^{13}C NMR (126 MHz, 298 K, DMSO-d_6): δ 156.4, 151.4, 148.2, 125.1, 121.8 (s, 10C, bpy), 124.4 (q, J_{FC} = 280.4 Hz, 2C, –CF$_3$), 71.7 (s, 2C, bpy-CH$_2$), 67.2 (q, J_{FC} = 33.4 Hz, 2C, –CH$_2$CF$_3$). ^{19}F NMR (470.5 MHz, 298 K, DMSO-d_6): δ −73.1 (t, J_{HF} = 8.6 Hz, 6F, –CH$_2$$CF_3$). FT-IR 1624, 1559, 1432 (m, bpy-ring), 1171, 1156 (s, CF_2 stretch). HR-FAB (M^+) $C_{16}H_{14}F_6N_2O_2Pt^{35}Cl_2$, calcd: m/z 644.9983, found: m/z 644.9984. $C_{16}H_{14}F_6N_2O_2Pt^{35}Cl^{37}Cl$, calcd: m/z 646.9957, found: m/z 646.9955. $C_{16}H_{14}F_6N_2O_2Pt^{37}Cl_2$, calcd: m/z 648.9950, found: m/z 648.9925. mp: decomposed at 208 °C before melting.

2.2.2. Preparation of Pt-4F (3)

Analytical data of ***Pt-4F*** *(**3**): Yield* 95.2%. ^{1}H NMR (500 MHz, 298 K, DMSO-d_6): δ 9.40 (dd, J_{HH} = 6.04 Hz, 2H, H_6), 8.42 (s, 2H, H_3), 7.78 (dd, J_{HH} = 6.04 Hz, 2H, H_5), 6.64 (tt, J_{FH} = 50.3 Hz, J_{FH} = 5.5 Hz, 2H, –CF$_2$$H$), 4.86 (s, 4H, bpy-C$H_2$), 4.16 (t, J_{FH} = 14.83 Hz, 4H, –CH_2CF$_2$CF$_2$H). ^{13}C NMR (126 MHz, 298 K, DMSO-d_6): δ 71 (bpy-CH_2O), 67.2 (bpy-CH$_2$OCH_2), 109.3–115.5 (CF_2)$_2$, 121.8, 125.1, 148.1, 151.5, 156.4 (bpy). ^{19}F NMR (470.5 MHz, 298 K, DMSO-d_6): δ −125.3 (m, –CH$_2$ CF_2CF$_2$, 4F), −140.1(d, CF$_2$$CF_2$H, 4F). FT-IR 1624, 1561, 1429 (m, bpy-ring), 1233, 1203, 1115 (m, CF_2 stretch). HR-FAB (M^+) $C_{18}H_{16}F_8N_2O_2Pt^{35}Cl_2$, calcd: m/z 709.0109, found: m/z 709.0114. $C_{18}H_{16}F_8N_2O_2Pt^{35}Cl^{37}Cl$, calcd: m/z 711.0079, found: m/z 711.0079. $C_{18}H_{16}F_8N_2O_2Pt^{37}Cl_2$, calcd: m/z 713.0050, found: m/z 713.0062. mp: decomposed at 230 °C before melting.

2.2.3. Preparation of Pt-5F (4)

Analytical data of ***Pt-5F*** *(**4**):* yield 84.2%. ^{1}H NMR (500 MHz, 298 K, DMSO-d_6): δ 9.40 (d, J_{HH} = 6.4 Hz, 2H, H_6), 8.37 (s, 2H, H_3), 7.74 (d, J_{HH} = 6.4 Hz, 2H, H_5), 4.90 (s, 4H, bpy-CH_2), 4.39 (t, J_{FH} = 14.0 Hz, 4H, –OCH_2CF$_2$). ^{13}C NMR (126 MHz, 298 K, DMSO-d_6): δ 156.4, 151.3, 148.2, 125.0, 121.5 (s, 10C, bpy), 118.5 (qt, J_{FC} = 282.6 Hz, J_{FC} = 31.2 Hz, 2C, –CF$_2$$CF_3$), 113.3 (tq, J_{FC} = 251.5 Hz, J_{FC} = 38.9 Hz, 2C, –CF$_2$CF$_3$), 71.1 (s, 2C, bpy-CH$_2$), 66.4 (t, J_{FC} = 25.6 Hz, 2C, -CH$_2$CF$_2$). ^{19}F NMR (470.5 MHz, 298 K, DMSO-d_6), δ −83.1 (s, 6F, –CF$_2$$CF_3$), −123.1 (t, J_{HF} = 15.1 Hz, 4F, –CF$_2$CF$_3$). FT-IR 1626, 1562, 1430 (m, bpy-ring), 1203, 1155 (s, CF_2 stretch). HR-FAB (M^+) $C_{18}H_{14}F_{10}N_2O_2Pt^{35}Cl_2$, calcd: m/z 744.9935, found: m/z 744.9920, $C_{18}H_{14}F_{10}N_2O_2Pt^{35}Cl^{37}Cl$, calcd: m/z 746.9893, found: m/z 746.9891, $C_{18}H_{14}F_{10}N_2O_2Pt^{37}Cl_2$, calcd: m/z 748.9875, found: m/z 748.9861. mp: decomposed at 221 °C before melting.

2.2.4. Preparation of Pt-7F (5) and Pt-8F (6)

Complexes **5** and **6** were prepared under the similar pathways described in previous report.[48]

2.3. Cell culture

Human breast carcinoma MCF-7, MDA-MB-231 cell lines and lung carcinoma A549 cell line were obtained from Bioresource Collection and Research Center (BCRC 60436, 60425 and 60074, respectively), Food Industry Research and Development Institute, Hsinchu, Taiwan. Human breast carcinoma MCF-7, MDA-MB-231 cells and lung carcinoma A549 cells were maintained in Dulbecco's modified Eagle's medium (DMEM; HyClone) with 10% fetal bovine serum (FBS; Biological industries), 2 mM L-glutamine and antibiotics (containing 100 mg/L streptomycin, 100 U/mL penicillin G, and 0.25 mg/L amphotericin B). Cells were maintained in a humidified incubator without/with 5% CO_2 at 37 °C.

Mammary epithelial M10 cell line was obtained from Bioresource Collection and Research Center (BCRC 60197) and maintained in Minimum Essential Medium (MEM; Gibco BRL) with 10% fetal bovine serum (FBS; Biological industries), 2 mM L-glutamine and antibiotics (containing 100 mg/L streptomycin, 100 U/mL penicillin G, and 0.25 mg/L amphotericin B). M10 cells were maintained in a humidified incubator with 5% CO_2 at 37 °C.

2.4. Cell viability assay

Cancer cells were seeded at a density of 1.5×10^4 cells per well in 96-well culture plates. After 24 h incubation, the cells were treated with different concentrations of compounds or DMSO as vehicle control for 48 h. Following cells were incubated with 3-(4,5-dimethylthiazol-2-yl)-2,5-diphenyltetrazolium bromide (1 mg/mL, MTT, Sigma) at 37 °C for 4 h. Then MTT-formazan product was dissolved by the addition of DMSO at room temperature for 30 min. The spectrophotometric absorbance of purple formazan, proportional to the number of viable cells, was determined by Molecular Devices SPECTRAmax PLUS^{384} at 540 nm.

2.5. Flow cytometry analysis

MDA-MB-231 cells were treated without/with complex **4** (12.5, 25 μM) for 24 and 48 h, respectively. Then the cells were harvested, fixed in cold 70% ethanol for at least 1 h at −20 °C, and resuspended in 1 mL PBS. The cell suspensions were treated with propidium iodide (PI) staining solution mix, 200 μg/mL RNase A, 0.1% Triton X-100 and 20 μg/mL PI, in the dark for 30 min, and then the cells were analyzed by using a FACSCalibur™ (Becton Dickinson, San Jose, CA). The cell cycle distribution was analyzed using ModFit LT software.

2.6. UV–Vis absorption spectroscopy

The salmon sperm DNA and cisplatin were purchased form Sigma. The ssDNA was rehydrated in deionized water and stored at 4 °C. The reactions were performed in a 3 mL cuvette at 25 °C. Briefly, different concentrations of cisplatin/DNA or complex **4**/DNA were mixed in deionized water solution and incubated at 37 °C for 2 h. The absorbance of each mixture was measured from 220 to 350 nm. During the DNA binding experiments, the concentration of DMSO in each cuvette was less than 0.1%. The effect of compound on UV absorption was subtracted consecutively by using different concentrations of compound in 0.1% DMSO reaction buffer as the blank sample. The final concentration of salmon sperm DNA was 25 ng/μL.

2.7. Gel mobility assay

Plasmid pSecTag2/Hygro B DNA was chosen for the assay. The reaction was performed by mixing various concentrations of cisplatin or complex **4** with 1 μg of pSECTag 2/Hygro B plasmid DNA in 20 μL of deionized water. The DMSO was controlled under 0.1% in the mixture. Assay solution was incubated at 37 °C for 24 h. The complex-DNA mixtures were loaded onto the 1% agarose gel and electrophoresis was carried under 1×TAE buffer (0.05 M Tris base, 0.05 M glacial acetic acid, 1 mM EDTA, pH 8.0) for 30 min and photographed in UV light.

2.8. Calculation of *c* log *P*

c log *P* values were predicted using ChemBioDraw Ultra 11.0 software.

3. Results

The preparation of ligands **a–e** started from deprotonation of readily available fluorinated alkanols (Scheme 1). Thus, R_fCH_2OH (R_f = CF_3, HC_2F_4, C_2F_5, C_3F_7 or HC_4F_8) was each treated with 30%

CH_3ONa/CH_3OH to give the corresponding alkoxides.[45–47] By pumping away the methanol, the resulting alkoxide was isolated as the salt. Then the nucleophilic attack by the moisture-sensitive alkoxide on 4,4′-bis($BrCH_2$)-2,2′-bpy in the dry solvent (e.g., THF) gave rise to the synthesis of bpy ligand, [4,4′-bis($R_fCH_2OCH_2$)-2,2′-bpy)] (**a**–**e**). The platinum complexes, **2**–**6**, were then easily synthesized by stirring the given ligand and metal precursor [$Pt(CH_3CN)_2Cl_2$], at an elevated temperature overnight (Scheme 1). Single crystals of the complexes **2**, **5**[48] and **6**[48] were grown by diffusion crystallization. Both the structures of **5** and **6** have been reported before.[48] The selected bond lengths and bond angles of complex **2** are listed in Figure 1. The first metal sphere shows the normal bond lengths and bond angles around the square planar Pt center. However, the orientation of the polyfluorinated ponytails of **2** is different from that of **5** or **6**. As shown in the Figure 1, the schematic drawing indicates that the two ponytails of **2** are bent toward each other. In contrast, the two ponytails of **5** and **6** are oriented to the other way so that their longer ponytails can avoid colliding with each other.

In addition, the intramolecular five-membered C–H···O hydrogen bonding system of **2**, **5**, and **6** is schematically shown and compared in Figure 2. Due to the less hindered CF_3 group, the O atom from **2** intramolecularly forms five-membered hydrogen bonding with the H3 atom. In contrast, O atom from complex **5** (or **6**) which has a longer group, C_3F_7 or HC_4F_8, forms the intramolecular five-membered hydrogen bonding with the H5 atom to avoid the steric hindrance from two $-CH_2OCH_2R_f$ groups. However, these polyfluorinated ponytails are able to have several weak interactions[47] with methylene and bipyridyl hydrogens in the neighboring molecules. From other related structures and their studies,[48] we think that the arrangement of the ponytails from **3** and **4** in the solid state should be, due to the steric reason, more similar to that of **5** or **6** than to that of **2**. However, the steric structure of the compound in solid state might not represent that of complex in the physiological condition, where it interacts with its biological partners including DNA.

The in vitro cytotoxic activity of the polyfluorinated bipyridine cisplatins **2–6** (Chart 1) against a panel of human cancer cell lines, MCF7 (breast adenocarcinoma), MDA-MB-231 (breast adenocarcinoma) and A549 (lung adenocarcinoma), is compared in Table 1. Cisplatin was used as our reference standard for comparison. Strikingly, complexes **2** and **4** having three and five fluorine atoms at each side chain showed uniquely specific antiproliferation effect against MDA-MB-231 cells with IC_{50} values of 16.5 and 12.5 μM,

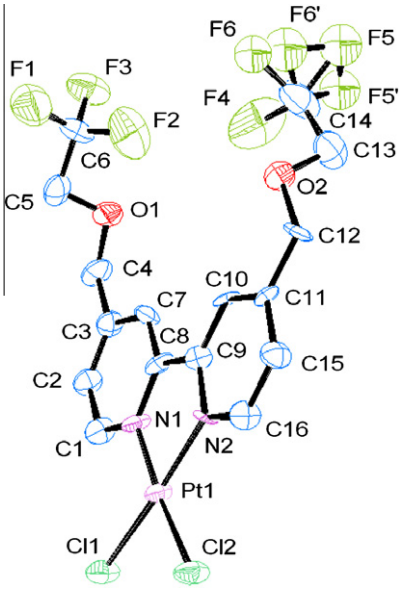

Figure 1. Molecular structure of the platinum complex **2** which shows one CF_3 group disordered, displacement ellipsoids drawn at the 40% probability level and all H atoms omitted. Selected bond lengths [Å] and angles [°] from its first metal sphere: Pt1–N(1) 2.000(11), Pt1–N(2) 1.987(10), Pt1–Cl(1) 2.303(4), Pt1–Cl(2) 2.300(4); N(1)–Pt1–N(2) 81.3(5), N(1)–Pt1–Cl(1) 94.3(4), N(1)–Pt1–Cl(2) 175.6(4), N(2)–Pt1–Cl(1) 175.6(3), N(2)–Pt1–Cl(2) 94.3(3), Cl(1)–Pt1–Cl(2) 90.1(1).

respectively, but they became significant loss of activity against two other cell lines at concentration of 20 μM (inhibiting MCF7 and A549 cells growth at the maximum of 5–18%, Table 1). Complex **3**, which bear four fluorine atoms at each side chain, gave promising results in inhibition of cell growth against both MCF7 and MDA-MB-231 cell lines with IC_{50} values of 59.5 and 19.2 μM while the potency of **3** against A549 cells resembled those of complexes **2** and **4**. It is interesting to note that complexes **5** and **6**, bearing the long polyfluorinated (seven and eight fluorine atoms) side chains, displayed weaker growth-inhibitory activity in comparison with complexes **2**–**4** against human MDA-MB-231 cancer cell line. Extended cytotoxic assays showed that complexes **5** and **6** had insignificant activity against both MCF7 and A549 cell lines at concentration of 20 μM (Table 1). On the basis of these observations, the restricted length of polyfluorinated side chain with three

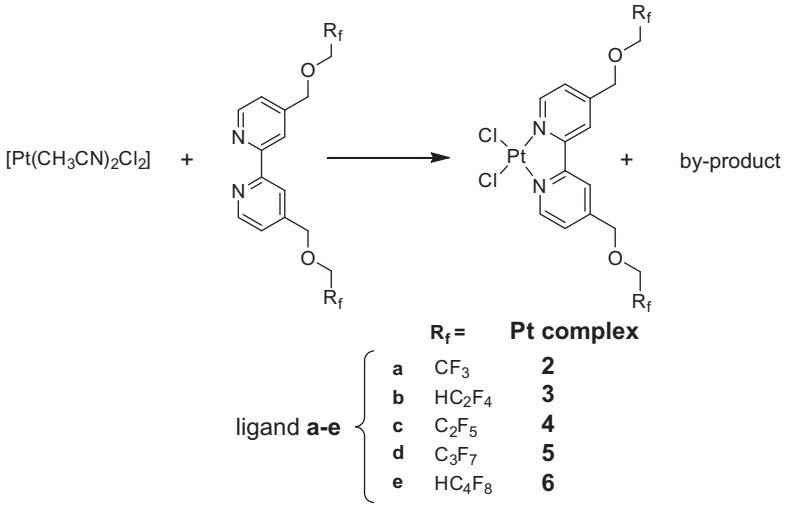

Scheme 1. Synthesis of platinum complexes **2**–**6**.

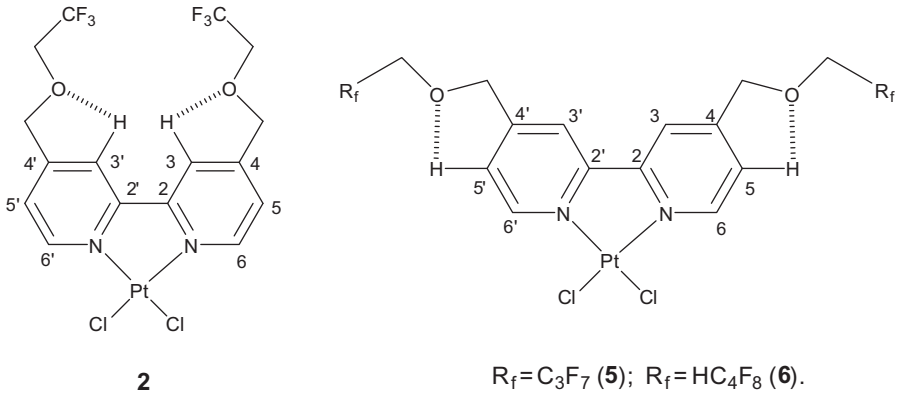

2

$R_f = C_3F_7$ (**5**); $R_f = HC_4F_8$ (**6**).

Figure 2. (left) The molecular structure of complex **2** forming five-membered O···H–C H-bonding with the H atom at 3 (or 3′) position; (right) due to the bulky R_f-containing ponytails, the O atom from the structure on the right forms the five-membered O···H–C H-bonding with the H atom at 5 (or 5′) position (**5** and **6**).

Table 1
Cytotoxicity of complexes **2**–**7** and cisplatin on three human cancer cell lines and the normal human breast epithelium cell line (M10)

Complex	IC_{50}[a] (μM)				SI[b]
	MCF-7	MDA-MB-231	A549	M10	
Cisplatin (**1**)	25.8 ± 0.6 (44)	31.0 ± 2.7 (27)	32.0 ± 3.2 (29)	29.0 ± 3.1 (50)	0.9
2	–(8)	16.5 ± 0.1 (78)	–(5)	30.7 ± 2.7 (0)	1.9
3	59.5 ± 5.9 (25)	19.2 ± 0.2 (53)	–(9)	41.0 ± 3.0 (3)	2.1
4	–(18)	12.5 ± 0.6 (83)	–(5)	–(0)[c]	>4
5	–(3)	–(0)	–(14)	–(11)	–
6	–(13)	–(9)	–(25)	–(46)	–
7	–(13)	–(38)	–(12)	–(19)	–

[a] Amount of cisplatin, polyfluorinated bipyridine cisplatins (**2**–**6**) and non-fluorinated bipyridine cisplatin (**7**) necessary to inhibit the growth of breast adenocarcinoma (MCF-7/MDA-MB-231), lung adenocarcinoma (A549) and normal breast epithelium cell (M10) by 50% in 48 h. Data are means ± SD (n = 3). The % inhibition, in parentheses, at 20 μM is expressed as the % inhibition of cell growth.

[b] Selectivity index = $IC_{50,M10}/IC_{50,MDA\text{-}MB\text{-}231}$.

[c] The % inhibition, in parentheses, at 50 μM is expressed as the % inhibition of cell growth.

to five fluorine atoms was evidently required for specific antiproliferation effect against the MDA-MB-231 cancer cell line. It is important to note that complexes **2**–**4** display greater antiproliferative activities than **7** against MDA-MB-231 cancer cell line, suggesting that the cytotoxicity perhaps is caused by fluorine-effects (Table 1).

The most active polyfluorinated bipyridine cisplatin **4**, possessing a high specificity for human MDA-MB-231 cancer cell line, exhibits a 2.5-fold potency increase over cisplatin (IC_{50} = 31.0 μM), a chemotherapeutic drug widely used in cancer treatments (Table 1). Similarly, complexes **2** and **3** exhibit a slight 1.6- to 2.0-fold potency increase over cisplatin. In contrast, complexes **2**–**6** no significant cytotoxicity was observed against both MCF7 and A549 cell lines, whereas cisplatin moderately inhibited cell growth with IC_{50} values of 25.8 and 32.0 μM, respectively.

Building on these cytotoxic data, we extended our studies further to the selectivity of polyfluorinated bipyridine cisplatins for malignant versus normal cells. Selective cytotoxicity of malignant cells rather than normal cells is important for the usefulness of anticancer agent in the treatment of cancer to sustain survival rates. The normal human breast epithelium cell line, M10, was chosen as a negative control to provide an evaluation of selectivity for malignant cells. As shown in Table 1, complex **2** was as cytotoxic as complex **3** to the MDA-MB-231 cancer cell line but almost 2-fold less toxic to normal M10 cell line. An analysis of cytotoxicity indicated that, to our surprise, complex **4** was 4-fold more active on MDA-MB-231 cells compared to M10 cells, whereas cisplatin was much more toxic toward normal M10 cells than complex **4**.

Understanding the mechanism of its cytotoxicity is biologically important with potential biomedical applications of metallodrug. Complex **4** was the most active and selective compound against the MDA-MB-231 cancer cell line, representing a practical candidate to gain insight about its mode of action. To probe whether the inhibition of breast adenocarcinoma proliferation of complex **4** associated with the alterations in cell cycle progression, MDA-MB-231 cells were incubated in the absence and presence of **4** (12.5 or 25.0 μM) for 24 h (Fig. 3, panel A) and 48 h (Fig. 3, panel B), respectively, followed by cell cycle distribution analysis by flow cytometry. Compared with untreated control cells, cells stimulated with complex **4** at 24 h showed a decrease in the percentage of cells in G_1 and an increase in the proportion of cells in S phase associated with a concomitant increase in the population of cells in G_2/M phase (Fig. 3, panel A). Furthermore, complex **4** treatment resulted in a significant inhibition of cell cycle progression in MDA-MB-231 cells at 48 h (Fig. 3, panel B), indicating evidence of complex **4**-induced S-G2/M arrest of human breast cancer cells. In particular, induction of apoptosis by complex **4** was validated by the occurrence of an apoptotic population in the sub-G1 phase at 24 and 48 h (Fig. 3, panels A and B).

DNA-binding studies on cisplatin have been broadly investigated including both intrastrand and interstrand DNA crosslinks.[49] The mechanism for cisplatin mediated anticancer action remains ambiguous. It is most likely that formation of bifunctional DNA–cisplatin adducts to unwind DNA is responsible for cytotoxicity.[50–54] Therefore, we chose to explore the binding mode of DNA with complex **4** using UV–Vis absorption spectroscopy and gel mobility assay. UV–Vis absorption spectral titrations were performed under a constant concentration of DNA (25 ng/μL) in the presence of different concentrations of cisplatin or complex **4**. Cisplatin was found to interact with salmon sperm DNA (ssDNA) in a fashion of slowly hyperchromic effect with a bathochromic shift

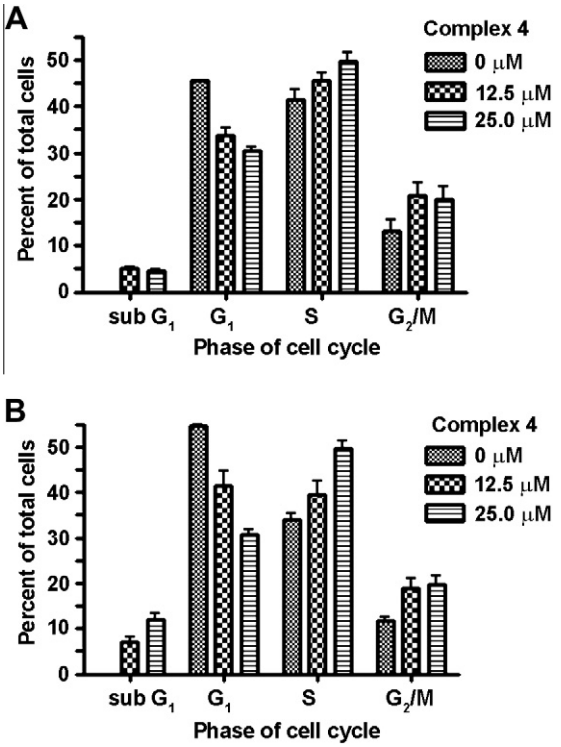

Figure 3. Complex **4** induced cell cycle arrest in human breast cancer cells. MDA-MB-231 cells were treated in the absence and presence of complex **4** (0, 12.5 and 25.0 μM) for (A) 24 h or (B) 48 h, respectively, and stained with propidium iodide followed by FACS analysis.

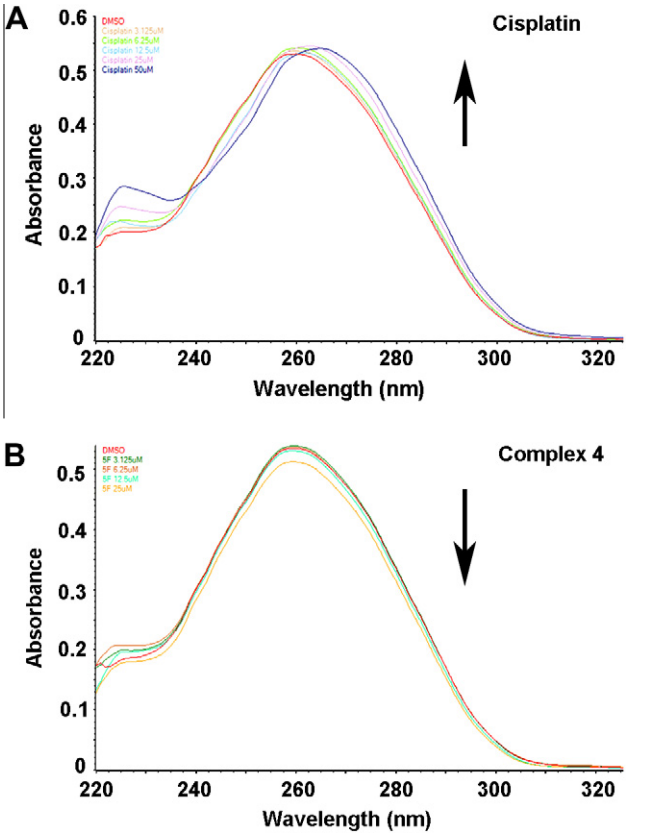

Figure 4. UV–visible absorption spectra for the titration of DNA with cisplatin (3.125, 6.25, 12.5, 25 and 50 μM) (panel A) and complex **4** (3.125, 6.25, 12.5 and 25 μM) (panel B), respectively. Arrow shows the absorbance changes upon increasing cisplatin or complex **4** concentrations.

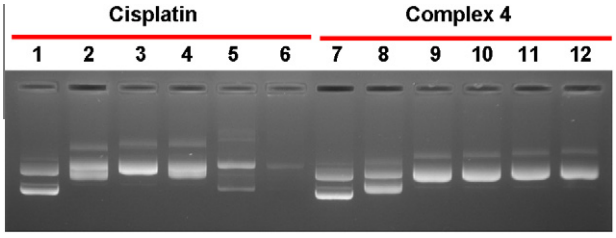

Figure 5. Analysis of gel electrophoretic mobility of pSecTag2/Hygro B plasmid DNA in the presence of cisplatin or complex **4** at different concentrations. Lanes 1 and 7, untreated pSecTag2/Hygro B plasmid DNA; lanes 2 and 8, 3.125 μM; lanes 3 and 9, 6.25 μM; lanes 4 and 10, 12.5 μM; lanes 5 and 11, 25 μM; lanes 6 and 12, 50 μM.

(Fig. 4A). However, upon the addition of ssDNA, complex **4** exhibited hypochromism without a bathochromic shift (Fig. 4B). Furthermore, the gel mobility assay was conducted to measure the DNA movement by using pSECTag 2/Hygro B plasmid DNA with increasing concentrations (3.125, 6.25, 12.5, 25, and 50 μM) of cisplatin and complex **4** (Fig. 5). Two main bands, open circular form and covalent closed circular form, of pSECTag 2/Hygro B plasmid DNA were observed in the electrophoretogram as the control (lanes 1 and 7 in Fig. 5). The covalent closed circular form usually moves faster due to its compact structure. At low concentrations of complex **4** and cisplatin (lanes 8, 9, 2, and 3 in Fig. 5), significant comigration of open circular form and covalent closed circular form was detected. In addition, a coalescence of two main bands was observed with complex **4** and cisplatin at the concentration range tested (lanes 9 and 3 in Fig. 5). At high concentrations of cisplatin (lanes 4, 5, and 6 in Fig. 5), a strong unwinding of negative supercoiled DNA to positive supercoiled DNA was displayed, whereas the same binding mode with complex **4** was not observed (lanes 10, 11 and 12 in Fig. 5).

c log *P* value is an important lipophilic parameter associated with prediction of drug-like physical properties in ADME (adsorption, distribution, metabolism and excretion) models. Recent studies have showed that *c* log *P* is also employed for explanations of inhibitory variation in enzyme activity,[55] difference in microsomal binding[56] and discrepancy in toxicological outcome in vivo.[57] The polyfluorinated bipyridine cisplatins **2** (three fluorine atoms), **3** (four fluorine atoms), **4** (five fluorine atoms), **5** (seven fluorine atoms) and **6** (eight fluorine atoms) have *c* log *P* of 6.26, 6.06, 8.29, 9.46, and 5.91 (Table 2),[58] respectively, indicating a positive correlation between lipophilicity and the number of fluorine atoms. In particular, the replacement of terminal fluorine atom with hydrogen atom leads to the reduction of lipophilicity (i.e., complexes **3** and **6**, Chart 1). Among those, complexes **2** and **4** showed the highest antiproliferation effects against MDA-MB-231 cells (IC_{50} values of 16.5 and 12.5 μM) and increased *c* log *P* values with respect to complex **3** or cisplatin. However, the dependence of antiproliferation effect on lipophilicity becomes ambiguous when complexes **5** and **6** have the low cytotoxicities (0% and

Table 2
c log *P* values of complexes **2**–**6** and cisplatin

Complex	Cisplatin (**1**)	**2**	**3**	**4**	**5**	**6**	Carboplatin
MW[a]	299	645	709	745	845	909	371
c log *P*	−2.5 (−1.68)[b]	6.26	6.06	8.29	9.46	5.91	−0.3 (−0.3)[b]

[a] Molecular weight.
[b] Data taken from Kitada et al.[58]

9% potency in the presence of 20 μM of **5** and **6**) but the maximal *c* log *P* (9.46) and the minimal *c* log *P* (5.91), respectively.

4. Discussion

Due to their structural similarity, the polyfluorinated bipyridine cisplatins **2–6** would be expected to behave in a comparable fashion in cytotoxicity. Our cytotoxic studies have revealed that most polyfluorinated bipyridine cisplatins exhibited specific selectivity toward human MDA-MB-231 cell line rather than other cancer cell lines, MCF-7 and A549. For example, MDA-MB-231 cells were particularly sensitive to complexes **2–4** (with IC_{50} values generally falling in the low micromolar range). For polyfluorinated bipyridine cisplatin complexes, the experimental significance of antiproliferation effect against MDA-MB-231 cells follows the trend: **4** > **2** > **3** > cisplatin >> **5**, **6**. Furthermore, these complexes were evaluated for their selectivity against MDA-MB-231 cells over normal human breast epithelium cell line M10 by calculating their selectivity index (SI, Table 1). Complex **4** has the best selectivity index (>4) among the polyfluorinated bipyridine cisplatins studied herein and the relative order of selectivity index is **4** > **3** > **2** > cisplatin, apparently similar to the tendency of antiproliferation effect. It is worth noting that complexes **2–4** have two or three methylenes linking with different number of fluorine atoms to the ether backbone (Chart 1). For example, complex **2** has three fluorine atoms, whereas, complex **3** and **4** have four and five fluorine atoms, respectively. This variation in number of fluorine atoms raises an attractive question of whether or not there is a physical or functional reason to explain varying number of fluorine atoms in these polyfluorinated bipyridine cisplatins associated with biological activity. More specifically, does the number of fluorine atoms have an effect on lipophilicity manipulating cytotoxicity? A priori, one would assume that the number of fluorine atoms should be critical for increasing lipophilicity so as to improve metabolic stability and enhance the cellular uptake. Instead, the relative order of *c* log *P* (lipophilic parameter) of these complexes is **5** > **4** > **2** > **3** > **6** >> cisplatin, carboplatin and the lipophilicity–cytotoxicity trend is merely valid within certain restricted number of fluorine atoms, that is, between three and five fluorine atoms, suggesting perhaps that modification of local structure (Fig. 2) from the extra fluorine atoms of polyfluorinated bipyridine cisplatins (**5** and **6**) hampers the interaction with their biological partners and prevails over lipophilicity in controlling cytotoxicity of complexes.

Complex **4**, which is the most active complex in the series, was found to be a more effective and selective anticancer agent than cisplatin. The latter induces the G_2/M arrest associated with DNA damage,[59] whereas the former represses the proliferation of MDA-MB-231 cells through the induction of S-G2/M arrest and apoptosis. A significant increase in the sub-G_1 cell population by complex **4** at 24 and 48 h is representative of cancer cells with fragmented DNA. These findings are consistent with the reported effects of new cisplatin analogues containing benzimidazole ligands, which significantly induce an increase in the sub-G1 cell population at a concentration of 20 μM.[50] The interactions of polyfluorinated bipyridine cisplatins to non-DNA and DNA targets appear to be the reasons for their mechanism of cytotoxicity, which then stimulates cancer cell death through apoptosis (or necrosis). Little is known about the binding mode of polyfluorinated bipyridine cisplatin–DNA interaction by which perhaps complex **4** induces cytotoxicity at the earlier stage of the cell cycle, followed by progress to the G_2/M phase to start the cell death program. It is clear from UV–Vis absorption titration studies that complex **4** triggers hypochromic effect of DNA with no obvious bathochromic shift, which is attributed to a partial intercalation. These results suggest that binding of complex **4** with DNA relies on proper electrostatic interaction through the phosphate group as described by Yang and Guo.[60] Furthermore, the decrease in the mobility of the DNA in the presence of low concentration of complex **4** was observed in the electrophoretograms (lane 8 in Fig. 5), indicating that the DNA–DNA cross-linking mediated by complex **4** can not be excluded. In contrast, cisplatin causes DNA hyperchromism with a bathochromic shift, suggesting the interaction with DNA bases and perhaps the damage of DNA structure.

The chemical structure of complex **2** is similar to that of cisplatin analog dichloro[4,4′-bis(4,4,4-trifluorobutyl)-2,2′-bipyridine]platinum (**8**) in the Ref. 27 (Chart 1) with a difference in one of the methylene group but oxygen atom in the fluorinated ponytails. It is interesting to note that a minor alteration of structure causes several discrepancies in biological properties. For example, complex **2** exhibits a 4-fold specificity (against MDA-MB-231 cells rather than A549 cells) increase over **8**,[27] indicating perhaps that insertion of the oxygen atom of **2** is tunable to the antiproliferative effect of different cancer cell lines. Complex **4** (two more fluorine atoms in each ponytails compared to complex **2**) suppresses the proliferation of MDA-MB-231 cells through the induction of S-G2/M arrest. In contrast, complex **8** blocks the MDA-MB-231 cells in both the G1 and S phases leading to a decrease in the G2 phase compared to that in the control.[27] Overall, these observations suggest that a minor structure difference in bipyridine cisplatin complexes (Chart 1) does impact their biological functions including cellular specificity and cell cycle distribution.

In the electrophoretogram the complex **4** (or cisplatin)-treated pSECTag 2/Hygro B plasmid DNA, significant comigration of open circular form and covalent closed circular form was observed and a coalescence of two main bands was found subsequently at low concentrations. The modification of electrophoretic mobility of two main bands (pSECTag 2/Hygro B plasmid DNA) is believed to be a result of interaction between complex **4** (or cisplatin) and DNA, apparently consistent with the studies from UV–Vis absorption titration. A strong unwinding of negative supercoiled DNA to positive supercoiled DNA was detected at high concentrations of cisplatin, whereas the same binding mode with complex **4** was not observed. This spectroscopic behavior of complex **4** can be interpreted as evidence of no unwinding of the supercoiled DNA. However, complex **4** exhibits a 2.5-fold potency increase over cisplatin, suggesting that pathway of unwinding of the supercoiled DNA is not the key factor to determine cytotoxicity of polyfluorinated bipyridine cisplatins **2–6**. In the present study, it is reasonable to postulate that the mechanism of cytotoxicity of complex **4** against MDA-MB-231 cells is different from that of cisplatin. Regardless, the combination of polyfluorinated side chain and bipyridine ligand results in a system showing promising cytotoxicity, underscoring the value and potential of this approach to probe selective anticancer agents.

5. Conclusion

In summary, a series of polyfluorinated bipyridine cisplatins **2–4** that are able to discriminate MDA-MB-231 cells rather than MCF-7 and A549 cells was discovered. A correlation between the relative order of lipophilicity of the polyfluorinated bipyridine cisplatins **2–4** and their cytotoxicities is established. Complex **4**, which is the most active complex in the series, was found to be a more effective and selective anticancer agent than cisplatin. In particular, complex **4** appears to have its cytotoxicity in a manner apparently inconsistent with cisplatin, through partial intercalation to DNA, which subsequently leads to induction of S-G2/M arrest and apoptosis. Our studies have also revealed the importance of different number of fluorine atoms to the ether backbone for manipulating

cytotoxicity. Therefore, further fundamental studies on polyfluorinated compounds are particularly interesting for both understanding structure–activity relationship and developing prospective pharmaceutics.

Acknowledgments

We are grateful for funding from the National Science Council in Taiwan, Academia Sinica (Summit project) and National Taipei University of Technology.

Supplementary data

Supplementary data associated with this article can be found, in the online version, at doi:10.1016/j.bmc.2011.06.065.

References and notes

1. Hird, M. *Chem. Soc. Rev.* **2007**, *36*, 2070.
2. Angerer, J.; Ewers, U.; Wilhelm, M. *Int. J. Hyg. Environ. Health* **2007**, *210*, 201.
3. Blanco, E.; Rodriguez-Abreu, C.; Schulz, P.; Ruso, J. M. *J. Colloid. Interface Sci.* **2010**, *341*, 261.
4. Kim, Y. H.; Yoon, D. K.; Lee, E. H.; Ko, Y. K.; Jung, H. T. *J. Phys. Chem. B.* **2006**, *110*, 20836.
5. Nishikawa, E.; Yamamoto, J.; Yokoyama, H. *Chem. Commun.* **2003**, *7*, 420.
6. Fisch, M. R.; Kumar, S.; Litster, J. D. *Phys. Rev. Lett.* **1986**, *57*, 2830.
7. Torres, M. F.; Sales, P. S.; Rossi, R. H.; Fernández, M. A. *Langmuir* **2010**, *26*, 17858.
8. Gan, J.; El Bakkari, M.; Belin, C.; Margottin, C.; Godard, P.; Pozzo, J. L.; Vincent, J. M. *Chem. Commun.* **2009**, 5133.
9. Campbell, T. Y.; Vecitis, C. D.; Mader, B. T.; Hoffmann, M. R. *J. Phys. Chem. A.* **2009**, *113*, 9834.
10. Gentilini, C.; Evangelista, F.; Rudolf, P.; Franchi, P.; Lucarini, M.; Pasquato, L. *J. Am. Chem. Soc.* **2008**, *130*, 15678.
11. Massi, L.; Guittard, F.; Levy, R.; Géribaldi, S. *Eur. J. Med. Chem.* **2009**, *44*, 1615.
12. Masuda, J.; Nakahara, H.; Karasawa, S.; Moroi, Y.; Shibata, O. *Langmuir* **2007**, *23*, 8778.
13. Nishimoto, K.; Kim, S.; Kitano, Y.; Tada, M.; Chiba, K. *Org. Lett.* **2006**, *8*, 5545.
14. Tortosa-Estorach, C.; Ruiz, N.; Masdeu-Bultó, A. M. *Chem. Commun.* **2006**, 2789.
15. Nordström, A.; Apon, J. V.; Uritboonthai, W.; Go, E. P.; Siuzdak, G. *Anal. Chem.* **2006**, *78*, 272.
16. Li, Z.; Kesselman, E.; Talmon, Y.; Hillmyer, M. A.; Lodge, T. P. *Science* **2004**, *306*, 98.
17. Eignerová, B.; Sedlák, D.; Dracínský, M.; Bartunek, P.; Kotora, M. *J. Med. Chem.* **2010**, *53*, 6947.
18. Zhao, B.; Hu, G. X.; Chu, Y.; Jin, X.; Gong, S.; Akingbemi, B. T.; Zhang, Z.; Zirkin, B. R.; Ge, R. S. *Chem. Biol. Interact.* **2010**, *188*, 38.
19. Blazejewski, J. C.; Wilmshurst, M. P.; Popkin, M. D.; Wakselman, C.; Laurent, G.; Nonclercq, D.; Cleeren, A.; Ma, Y.; Seo, H. S.; Leclercq, G. *Bioorg. Med. Chem.* **2003**, *11*, 335.
20. Dunn, A. R.; Belliston-Bittner, W.; Winkler, J. R.; Getzoff, E. D.; Stuehr, D. J.; Gray, H. B. *J. Am. Chem. Soc.* **2005**, *127*, 5169.
21. de Leval, X.; Ilies, M.; Casini, A.; Dogné, J. M.; Scozzafava, A.; Masini, E.; Mincione, F.; Starnotti, M.; Supuran, C. T. *J. Med. Chem.* **2004**, *47*, 2796.
22. Youssef, J.; Badr, M. *Crit. Rev. Toxicol.* **1998**, *28*, 1.
23. Vanden Heuvel, J. P.; Kuslikis, B. I.; Shrago, E.; Peterson, R. E. *Biochem. Pharmacol.* **1991**, *42*, 295.
24. Shi, J.; Du, J.; Ma, T.; Pankiewicz, K. W.; Patterson, S. E.; Tharnish, P. M.; McBrayer, T. R.; Stuyver, L. J.; Otto, M. J.; Chu, C. K.; Schinazi, R. F.; Watanabe, K. A. *Bioorg. Med. Chem.* **2005**, *13*, 1641.
25. Wohlrab, F.; Jamieson, A. T.; Hay, J.; Mengel, R.; Guschlbauer, W. *Biochim. Biophys. Acta* **1985**, *824*, 233.
26. Sekine, T.; Takahashi, J.; Nishishiro, M.; Arai, A.; Wakabayashi, H.; Kurihara, T.; Kobayashi, M.; Hashimoto, K.; Kikuchi, H.; Katayama, T.; Kanda, Y.; Kunii, S.; Motohashi, N.; Sakagami, H. *Anticancer Res.* **2007**, *27*, 133.
27. Elwell, K. E.; Hall, C.; Tharkar, S.; Giraud, Y.; Bennett, B.; Bae, C.; Carper, S. W. *Bioorg. Med. Chem.* **2006**, *14*, 8692.
28. Kawase, M.; Sakagami, H.; Kusama, K.; Motohashi, N.; Saito, S. *Bioorg. Med. Chem. Lett.* **1999**, *9*, 3113.
29. Hoffmann-Röder, A.; Schoenhentz, J.; Wagner, S.; Schmitt, E. *Chem. Commun.* **2011**, *47*, 382.
30. Yoder, N. C.; Yüksel, D.; Dafik, L.; Kumar, K. *Curr. Opin. Chem. Biol.* **2006**, *10*, 576.
31. Galanski, M.; Jakupec, M. A.; Keppler, B. K. *Curr. Med. Chem.* **2005**, *12*, 2075.
32. Marcon, G.; Carotti, S.; Coronnello, M.; Messori, L.; Mini, E.; Orioli, P.; Mazzei, T.; Cinellu, M. A.; Minghetti, G. *J. Med. Chem.* **2002**, *45*, 1672.
33. Casini, A.; Cinellu, M. A.; Minghetti, G.; Gabbiani, C.; Coronnello, M.; Mini, E.; Messori, L. *J. Med. Chem.* **2006**, *49*, 5524.
34. Rajendiran, V.; Karthik, R.; Palaniandavar, M.; Stoeckli-Evans, H.; Periasamy, V. S.; Akbarsha, M. A.; Srinag, B. S.; Krishnamurthy, H. *Inorg. Chem.* **2007**, *46*, 8208.
35. Balakrishna, M. S.; Suresh, D.; Rai, A.; Mague, J. T.; Panda, D. *Inorg. Chem.* **2010**, *49*, 8790.
36. Gao, E.; Zhu, M.; Liu, L.; Huang, Y.; Wang, L.; Shi, C.; Zhang, W.; Sun, Y. *Inorg. Chem.* **2010**, *49*, 3261.
37. Mansouri-Torshizi, H.; I-Moghaddam, M.; Divsalar, A.; Saboury, A. A. *Bioorg. Med. Chem.* **2008**, *16*, 9616.
38. Bieda, R.; Ott, I.; Dobroschke, M.; Prokop, A.; Gust, R.; Sheldrick, W. S. *J. Inorg. Biochem.* **2009**, *103*, 698.
39. Karki, S. S.; Thota, S.; Darj, S. Y.; Balzarini, J.; De Clercq, E. *Bioorg. Med. Chem.* **2007**, *15*, 6632.
40. Zava, O.; Zakeeruddin, S. M.; Danelon, C.; Vogel, H.; Grätzel, M.; Dyson, P. J. *ChemBioChem* **2009**, *10*, 1796.
41. Gao, E. J.; Sun, T. D.; Liu, S. H.; Ma, S.; Wen, Z.; Wang, Y.; Zhu, M. C.; Wang, L.; Gao, X. N.; Guan, F.; Guo, M. J.; Liu, F. C. *Eur. J. Med. Chem.* **2010**, *45*, 4531.
42. Kumar, L.; Kandasamy, N. R.; Srivastava, T. S.; Amonkar, A. J.; Adwankar, M. K.; Chitnis, M. P. *J. Inorg. Biochem.* **1985**, *23*, 1.
43. Pucci, D.; Bellusci, A.; Bernardini, S.; Bloise, R.; Crispini, A.; Federici, G.; Liguori, P.; Lucas, M. F.; Russo, N.; Valentini, A. *Dalton Trans.* **2008**, 5897.
44. Vo, V.; Kabuloglu-Karayusuf, Z. G.; Carper, S. W.; Bennett, B. L.; Evilia, C. *Bioorg. Med. Chem.* **2010**, *18*, 1163.
45. Lu, N.; Tu, W. H.; Wu, Z. W.; Wen, Y. S.; Liu, L. K. *Acta Cryst. C.* **2010**, *66*, o289.
46. Lu, N.; Tu, W. H.; Wen, Y. S.; Liu, L. K.; Chou, C. Y.; Jiang, J. C. *Cryst. Eng. Comm.* **2010**, *12*, 538.
47. Lu, N.; Lin, Y. C.; Chen, J. Y.; Chen, T. C.; Chen, S. C.; Wen, Y. S.; Liu, L. K. *Polyhedron* **2007**, *26*, 3045.
48. Lu, N.; Hou, H. C.; Lin, C. T.; Li, C. K.; Liu, L. K. *Polyhedron* **2010**, *29*, 1123.
49. Keck, M. V.; Lippard, S. J. *J. Am. Chem. Soc.* **1992**, *114*, 3386.
50. Gümüş, F.; Eren, G.; Açik, L.; Celebi, A.; Oztürk, F.; Yilmaz, S.; Sagkan, R. I.; Gür, S.; Ozkul, A.; Elmali, A.; Elerman, Y. *J. Med. Chem.* **2009**, *52*, 1345.
51. Cohen, G. L.; Bauer, W. R.; Barton, J. K.; Lippard, S. J. *Science* **1979**, *203*, 1014.
52. Jamieson, E. R.; Lippard, S. J. *Chem. Rev.* **1999**, *99*, 2467.
53. Takahara, P. M.; Rosenzweig, A. C.; Frederick, C. A.; Lippard, S. J. *Nature* **1995**, *377*, 649.
54. Gelasco, A.; Lippard, S. J. *Biochemistry* **1998**, *37*, 9230.
55. Lewis, D. F. V.; Lake, B. G.; Ito, Y.; Dickins, M. *J. Enzyme Inhib. Med. Chem.* **2006**, *21*, 385.
56. Austin, R. P.; Barton, P.; Cockroft, S. L.; Wenlock, M. C.; Riley, R. J. *Drug Metab. Dispos.* **2002**, *30*, 1497.
57. Hughes, J. D.; Blagg, J.; Price, D. A.; Bailey, S.; Decrescenzo, G. A.; Devraj, R. V.; Ellsworth, E.; Fobian, Y. M.; Gibbs, M. E.; Gilles, R. W.; Greene, N.; Huang, E.; Krieger-Burke, T.; Loesel, J.; Wager, T.; Whiteley, L.; Zhang, Y. *Bioorg. Med. Chem. Lett.* **2008**, *18*, 4872.
58. Kitada, N.; Takara, K.; Tsujimoto, M.; Sakaeda, T.; Ohnishi, N.; Yokoyama, T. *J. Cancer Mol.* **2007**, *3*, 23.
59. Mueller, S.; Schittenhelm, M.; Honecker, F.; Malenke, E.; Lauber, K.; Wesselborg, S.; Hartmann, J. T.; Bokemeyer, C.; Mayer, F. *Int. J. Oncol.* **2006**, *29*, 471.
60. Yang, P.; Guo, M. *Coord. Chem. Rev.* **1999**, *185–186*, 189.